Chromosoma (2010) 119:41–58
DOI 10.1007/s00412-009-0243-3

RESEARCH ARTICLE

Synaptonemal complex stability depends on repressive histone marks of the lateral element-associated repeat sequences

Abrahan Hernández-Hernández · Rosario Ortiz · Ernestina Ubaldo · Olga M. Echeverría Martínez · Gerardo H. Vázquez-Nin · Félix Recillas-Targa

Received: 3 March 2009 / Revised: 7 September 2009 / Accepted: 21 September 2009 / Published online: 9 October 2009

Abstract The synaptonemal complex (SC) is the central key structure for meiosis in organisms undergoing sexual reproduction. During meiotic prophase I, homologous chromosomes exchange genetic information at the time they are attached to the lateral elements by specific DNA sequences. Most of these sequences, so far identified, consist of repeat DNA, which are subject to chromatin structural changes during meiotic prophase I. In this work, we addressed the effect of altering the chromatin structure of repeat DNA sequences mediating anchorage to the lateral elements of the SC. Administration of the histone deacetylase inhibitor trichostatin A into live rats caused death of cells in the pachytene stage as well as changes in histone marks along the synaptonemal complex. The most notable effect was partial loss of histone H3 lysine 27 trimethylation. Our work describes the epigenetic landscape of lateral element-associated chromatin and reveals a critical role of histone marks in synaptonemal complex integrity.

Electronic supplementary material The online version of this article (doi:10.1007/s00412-009-0243-3) contains supplementary material, which is available to authorized users.

A. Hernández-Hernández · R. Ortiz · E. Ubaldo · O. M. Echeverría Martínez · G. H. Vázquez-Nin (✉)
Laboratorio de Microscopía Electrónica,
Departamento de Biología Celular, Facultad de Ciencias,
Universidad Nacional Autónoma de México (UNAM),
México D.F. C.P. 04510, Mexico
e-mail: ghvn@hp.fciencias.unam.mx

A. Hernández-Hernández · F. Recillas-Targa (✉)
Instituto de Fisiología Celular,
Departamento de Genética Molecular,
Universidad Nacional Autónoma de México (UNAM),
Apartado Postal 70-242, México D.F. C.P. 04510, Mexico
e-mail: frecilla@ifc.unam.mx

Introduction

Meiosis is a specialized cell division process present in the organisms with sexual reproduction and that produces genetic variability by homologous chromosome recombination. Such recombination occurs in the context of the synaptonemal complex (SC), a proteinaceous structure that holds the chromosome axes of homologous chromosomes together until the exchange of genetic material is completed (Page and Hawley 2004). Chromatin of homologous chromosomes is anchored to the lateral elements (LEs) of the SC. Analysis of DNA associated with the synaptonemal complex protein 3 (SYCP3) demonstrated enrichment of repeat DNA sequences, which localize to the LEs, as well as in the bulk of the chromatin, as shown by in situ hybridization (Hernández-Hernández et al. 2008). Features in the primary structure of lateral element-associated repeat sequences (LEARS) did not reveal any obvious consensus sequence, suggesting that secondary structure might be responsible for recruitment of LEARS to the LEs. In somatic cells, most of these transcriptionally inactive repeat sequences are subject to epigenetic modification favoring their organization in heterochromatin (Martens et al. 2005). Furthermore, chromatin structure dictated by epigenetic modifications during meiosis is critical for accurate SC assembly and meiosis progression (Hernández-Hernández et al. 2009). Therefore, it is possible that specific epigenetic modifications of LEARS influence their interaction with LEs and subsequently affect the SC structure. In this work, we investigated the epigenetic profile of LEARS in the context of the SC by analyzing a subset of posttranslational histone modifications. Furthermore, we addressed the effect of in vivo inhibition of histone deacetylases on SC structure. Our results suggest that certain histone marks

are indeed needed for the anchorage of chromosomes to the LEs; moreover, the loss of the interaction between DNA and the LEs is accompanied by alteration of the SC's proteinaceous structure.

Material and methods

Animal care and treatment

Wistar adult male rats were split into groups A, B, and C, containing two rats each. Rats from group A were treated with 2.4 mg/kg of the histone deacetylase inhibitor trichostatin A (TSA, Sigma), which was administered daily by subcutaneous injection as previously reported (Fenic et al. 2004). TSA was dissolved in dimethylsulfoxide (DMSO; Sigma) to obtain a 20-mg/ml stock solution. Animals from group B received DMSO diluted in phosphate-buffered saline (PBS) without TSA and served as a control group, while group C represented untreated control animals. Animals were treated for 9 days, which corresponds to the time of leptotene to pachytene stage progression in the rat seminiferous cycle (Adler 1996). Therefore, the early and midpachytene cells found at the ninth day of treatment correspond to pachytene cell that have been treated daily since leptotene stage. Therefore, the cells at different stages of meiotic prophase I (i.e., zygotene and pachytene) at the beginning of treatment are not evaluated since they are in most advances rather than early and midpachytene at the end of the treatment. Rats were sacrificed, and their testes were excised and split to perform histochemistry, immunohistochemistry, electron microscopy analyses, and chromatin immunoprecipitation (ChIP) assays (Fig. S1). TSA dosage was chosen according to the previous data on TSA dosage effect in spermatogenesis. The TSA dosage used in this work allows for the evaluation of pachytene cells, as higher doses produce a 96% depletion of pachytene cells (Fenic et al. 2004). In the manipulation of the animals, we followed the ethical guidelines as recommended in the "Guide for Care and Use of Laboratory Animals" (National Research Council, (NRC) 1996).

Immunofluorescence and histochemistry

Testes were fragmented into small pieces and cryofixed with prechilled isopentane embedded in liquid nitrogen. Samples were sectioned immediately in a cryostat (Leica) and mounted in poly-L-lysine (Sigma)-treated slides. Immunolocalizations were performed in a humid chamber employing the following antibodies: anti-SYCP3, anti-SYCP1 (kindly provided by Ricardo Benavente), anti-H3K9me1, anti-H3K9me2, anti-H3K9me3, anti-H3K27me1, anti-H3K27me2, anti-H3K27me3, anti-H4K20me1, anti-H4K20me2, anti-H4K20me3 (some of which were kindly provided by Thomas Jenuwein, and the others were purchased from Abcam), anti-H2AXγ (Upstate), and anti-DMC1 (Abcam). Antibodies were diluted 1/200 in PBS. Primary antibodies were detected with fluorescein-coupled or Texas Red-coupled Alexa Fluor (Invitrogen). Secondary antibodies were used at a 1/200 dilution. Slides were counterstained with 100 μg/ml 4′,6-diamidino-2-phenylindole (DAPI). Slides were rinsed with PBS-Tween, mounted with Vectashield mounting medium (Vector) and analyzed in an Apotome-equipped microscope (Carl Zeiss). Optical sections were produced with the Axiovision software. For histochemistry, small fragments of testis were fixed in Bouin fixative and embedded in paraffin using standard techniques. Five micrometers paraffin sections were stained with hematoxylin and eosin.

Chromatin immunoprecipitation and re-ChIP

Chromatin immunoprecipitation was performed from testes as described (Hernández-Hernández et al. 2008). For the re-ChIP assay, briefly: a first chromatin immunoprecipitation was done with anti-SYCP3 antibody, and the immunocomplex was precipitated employing sepharose beads-coupled A/G proteins. Then the immunocomplex was washed as reported (Hernández-Hernández et al. 2008). Before DNA extraction and crosslink reversal, the immunocomplex was dissociated by adding 10 mM dithiothreitol, and the beads were pelleted and discarded. Subsequently, protein-DNA complexes were reimmunoprecipitated with 5 μg of the following antibodies: anti-H3 acetylated, anti-H3K9me3, anti-H3K27me3, and anti-H4K20me3. Next, immunocomplexes were pulled-down using sepharose bead-coupled A/G proteins and washed. The eluted DNA was employed as a template in radioactive polymerase chain reactions (PCRs) as previously reported (Hernández-Hernández et al. 2008).

Electron microscopy serial sections and preferential DNA staining

Rat seminiferous tubule fragments of 1 mm^3 were fixed in 2.5% glutaraldehyde for 1 h, rinsed with PBS, dehydrated, and embedded in epoxy resin. After 24 h of polymerization at 65ºC, the resin blocks were cut in an ultra microtome (Leica Instruments). Pachytene cells were determined according to the cellular associations of the cycle of seminiferous epithelium in semifine sections. Once the midpachytene cells were identified, the blocks were cut in ultrafine sections of approximately 60 nm in width. Sections were collected in Sjostrand nickel grids and mounted on a formvar film. Grids were split for

contrast methods. For general staining, the grids were contrasted with uranyl acetate for 10 min and lead citrate for 5 min. A total of 50 nuclei per experiment of TSA treatment were analyzed (n=150). Nuclei with altered SC structure were observed through the serial sections in the grid (at least 100 serial sections per grid). For specific DNA staining, sections were mounted in gold grids without formvar film, and we used the osmium-ammine procedure (Cogliati and Gautier 1973). Samples were observed in a transmission electron microscope (JEOL 1010).

Results

Epigenetic landscape of lateral element-associated repeat sequences

Homologous chromosomes are anchored to the LEs of the SC by several kinds of repeat DNA sequences (LEARS). The chromatin structure of these sequences could be involved in their recruitment to the SC and in the stability of this meiosis-specific structure (Hernández-Hernández et al. 2008). Hence, we decided to perform immunolocalization assays to identify the posttranslational histone marks associated with the SC. We used antibodies against histone marks associated with relaxed or compact chromatin configurations. Monomethylations of histone H3 at lysines 9 and 27 and of histone H4 at lysine 20 (H3K9me1, H3K27me1, and H4K20me1, respectively) are epigenetic marks associated with relaxed chromatin (Barski et al. 2007). In contrast, dimethylation of the same residues (H3K9me2, H3K27me2, and H4K20me2, respectively) is associated with facultative heterochromatin. Trimethylated states (H3K9me3, H3K27me3, and H4K20me3, respectively) are found in constitutive heterochromatin and in the majority of repeat elements (Martens et al. 2005; Barski et al. 2007). Our results indicate that the histone marks, H3K9me1, H3K27me1, H4K20me1, H3K9me2, H3K27me2, and H4K20me2, were absent from the SC core as visualized by the immunolocalization of SYCP3. However, they were found in the surrounding chromatin (Fig. 1a–l and a'–l'). Histone mark H3K9me2 was observed in the chromatin of the XY body as expected (data not shown) because of the presence of facultative heterochromatin in this structure (Khalil et al. 2004). The presence of H3K9me3 and H4K20me3 was evident by the appearance of foci that colocalized at the SC's extremity along the nuclear periphery, where the brightest SYCP3 signals were seen (arrows in Fig. 1a''–d'' and i''–l'', respectively). These brightest SYCP3 dots correspond to telomeres anchored to the adhesion plate in the nuclear envelope (NE; Viera et al. 2003). Finally, the signal of H3K27me3 colocalized with SYCP3 at several points along the LEs (arrows in Fig. 1e''–h'').

Dynamics of histone marks associated with the SC during meiotic prophase I

We observed that H3K9me3, H3K27me3, and H4K20me3 showed some colocalization with the signal of SYCP3 in midpachytene cells, which were identified according to the surrounding cellular associations and comparisons with the cycle of the seminiferous epithelium in rat (CSE; Clermont 1972). To analyze whether these associations were exclusive to the pachytene cells, we followed the dynamics of the three histone marks associated with the SC during early stages of the meiotic prophase I.

H3K9me3 was observed as foci that colocalized with the brightest signal of anti-SYCP3 antibody, which marked the telomere region of the newly formed axial elements (AE) in leptotene stage (Fig. 2a–d). At zygotene stage, the signal of this histone mark was present at telomere region (Fig. 2e–h). This association continued in early pachytene (Fig. 2i–l) and through midpachytene in the chromosome ends of the mature SC (Fig. 2m–p). Further, the signal of H3K27me3 was slightly visible in leptotene and zygotene stages (Fig. 3a–d and e–h, respectively), whereas at early pachytene, the signal was more evident and colocalized with the SC in scarce points (Fig. 3i–l). At midpachytene, the signal was yet more evident and colocalized with the SC in long stretches (Fig. 3m–p).

The H4K20me3 signal had a similar pattern to that present in the staining of H3K9me3, being present in foci that colocalized with the telomere region in leptotene and zygotene stages (Fig. 4a–d and e–h, respectively) and with the chromosome ends at early and midpachytene stages (Fig. 4i–l and m–p, respectively).

These results show that H3K9me3 and H4K20me3 were present in the telomere region of the AE until they mature into LE in the SC. The dynamics of these marks was seen in 100% of the analyzed cells throughout leptotene, zygotene, and pachytene (n=150, for each stage; Fig. 5). On the other hand, the signal for H3K27me3 was barely visible from leptotene to zygotene stages in 100% of the analyzed nuclei (Fig. 5). The signal became visible at early pachytene and colocalized with the newly formed SC in 70% of the analyzed nuclei. Towards midpachytene, 96% of the nuclei displayed colocalization of H3K27me3 with the mature SC (Fig. 5). These results suggest that H3K9me3 and H4K20me3 are constitutively in the chromatin that will become part of the SC extremity. H3K27me3 appeared to colocalize with the SC at the time the structure matures, suggesting a possible role in the formation and/or maintenance of the SC.

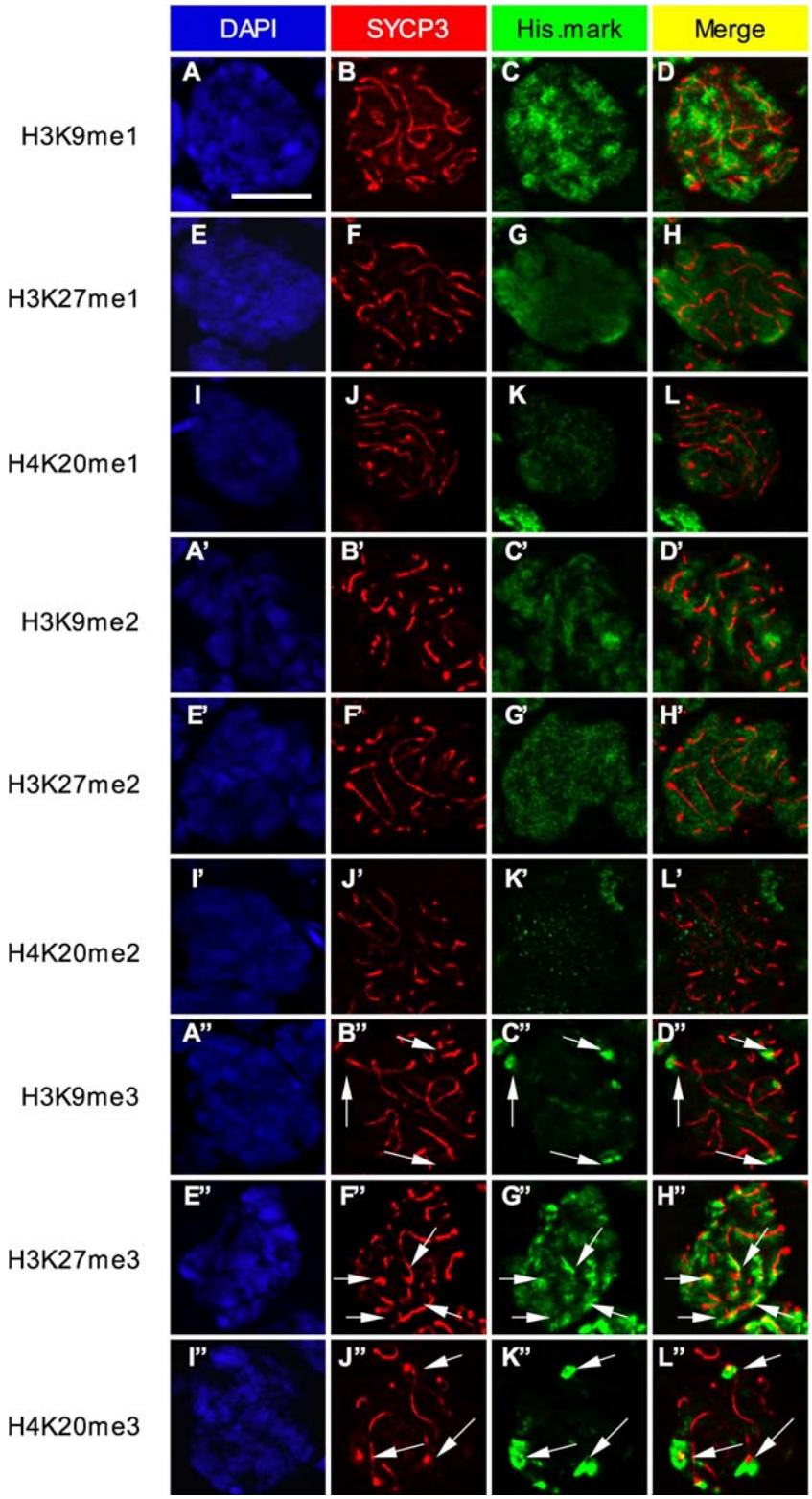

Fig. 1 Optical sections of midpachytene cells. Immunolocalization for the histone marks (*His.mark*) H3K9me1, H3K27me1, H4K20me1, H3K9me2, H3K27me2, H4K20me2, H3K9me3, H3K27me3, and H4K20me3 in midpachytene cells (*green*). SYCP3 immunodetection was used to indicate the SCs (*red*). Nuclei were stained with DAPI. Optical sections were made every 0.7 μm; therefore, not all SCs in pachytene nuclei are displayed. The *bar* corresponds to 10 μm

Histone deacetylase inhibition causes damage in pachytene cells

Histone deacetylases (HDACs) promote removal of acetyl groups from histone lysine residues, thus, allowing their methylation and driving the formation of specific chromatin configurations (Ekwall et al. 1997). It has been reported that inhibition of HDACs is associated with infertility, meiosis impairment, and arrest of meiocytes in the pachytene stage (Fenic et al. 2004,

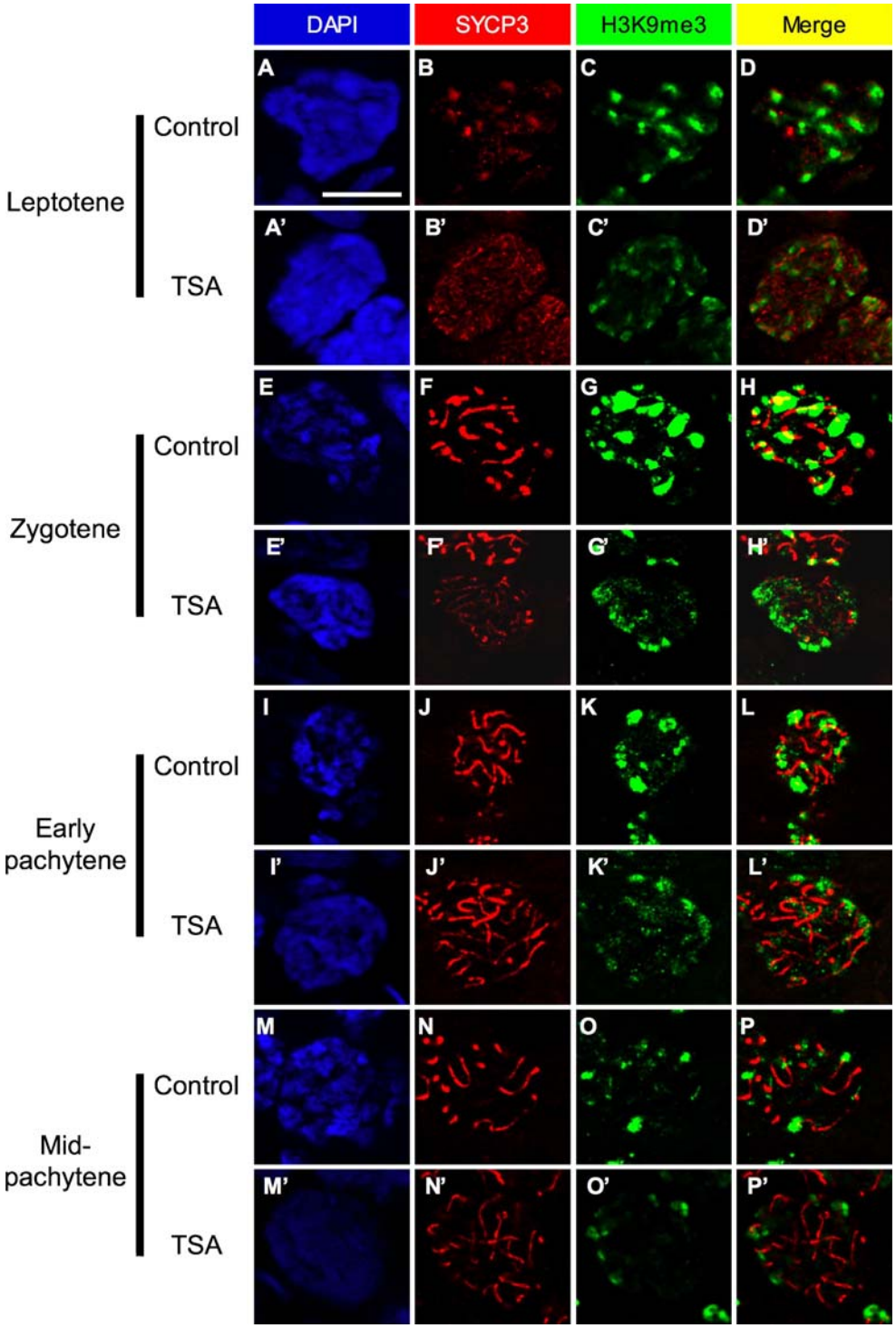

Fig. 2 Immunolocalization of histone mark H3K9me3 throughout meiotic prophase I of control and TSA-treated animals. SYCP3 immunodetection was used to indicate the SCs (*red*). Nuclei were stained with DAPI. **a**–**d** Leptotene cell from control animals. **a**'–**d**' Leptotene cell from TSA-treated animals. **e**–**h** Zygotene cell from control animals. **e**'–**h**' Zygotene cell from TSA-treated animals. **i**–**l** Early pachytene cell from control animals. **i**'–**l**' Early pachytene cell from TSA-treated animals. **m**–**p** Midpachytene cell from control animals. **m**'–**p**' Midpachytene cell from TSA-treated animals. The *bar* corresponds to 10 μm in all the optical sections

2008). Inhibition of HDACs impedes deacetylation and, therefore, methylation of histones, which interferes with the formation of heterochromatin (Ekwall et al. 1997), potentially affecting the formation of the SC. Since we found that H3K9me3, H4K20me3, and H3K27me3 colocalized with the SC and that dynamics of H3K27me3 suggest a potential role of this mark during the SC formation, we decided to inhibit HDAC activity through meiotic prophase I (see Material and methods). As a first approach, we tested whether inhibition of HDACs affect pachytene cells as previously reported (Fenic et al. 2004, 2008). To this end, we treated rats with TSA (Fenic et al. 2004, 2008) during meiotic prophase I and analyzed the morphology of the seminiferous tubules. As expected, meiotic cells in seminiferous tubules undergo apoptosis in the 40% of analyzed seminiferous tubules as shown

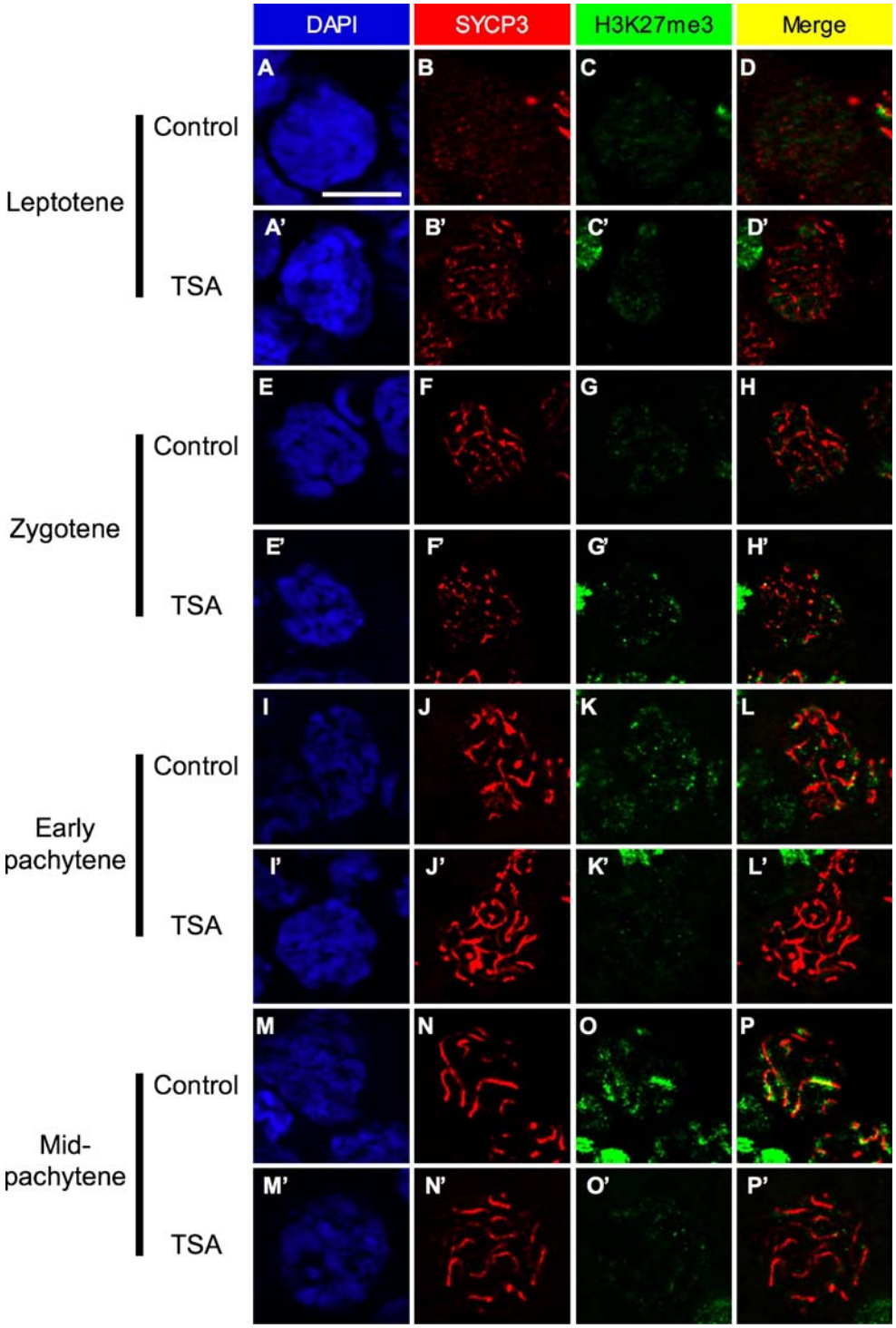

Fig. 3 Immunolocalization of histone mark H3K27me3 throughout meiotic prophase I of control and TSA-treated animals. SYCP3 immunodetection was used to indicate the SCs (red). Nuclei were stained with DAPI. **a–d** Leptotene cell from control animals. **a'**–**d'** Leptotene cell from TSA-treated animals. **e–h** Zygotene cell from control animals. **e'**–**h'** Zygotene cell from TSA-treated animals. **i–l** Early pachytene cell from control animals. **i'**–**l'** Early pachytene cell from TSA-treated animals. **m–p** Midpachytene cell from control animals. **m'**–**p'** Midpachytene cell from TSA-treated animals. The *bar* corresponds to 10 μm in all the optical sections

by TUNEL assay (Fig. S2A–F). To identify the affected cells, we analyzed histological sections of seminiferous tubules. Meiotic stages were identified according to the cell association of the CSE (Clermont 1972). During stage III of the CSE, cells in early pachytene stage and spermatids in stages 3 and 16 of spermiogenesis were visible in both control and treated rats (Fig. S2G–L). Interestingly, in treated rats, affected cells were identified in stage IX of the CSE in which spermatids in step 9 of spermiogenesis and midpachytene stage cells were present in control and treated rats (Fig. S2H, K). These results indicate that not all the early pachytene cells progress to mid pachytene stage in TSA-treated rats (asterisk in Fig. S2K). This was found in 76% of the observed seminiferous tubules (50 seminiferous tubules per experiment, $n=150$). In contrast, at stage XIII of the CSE, cells

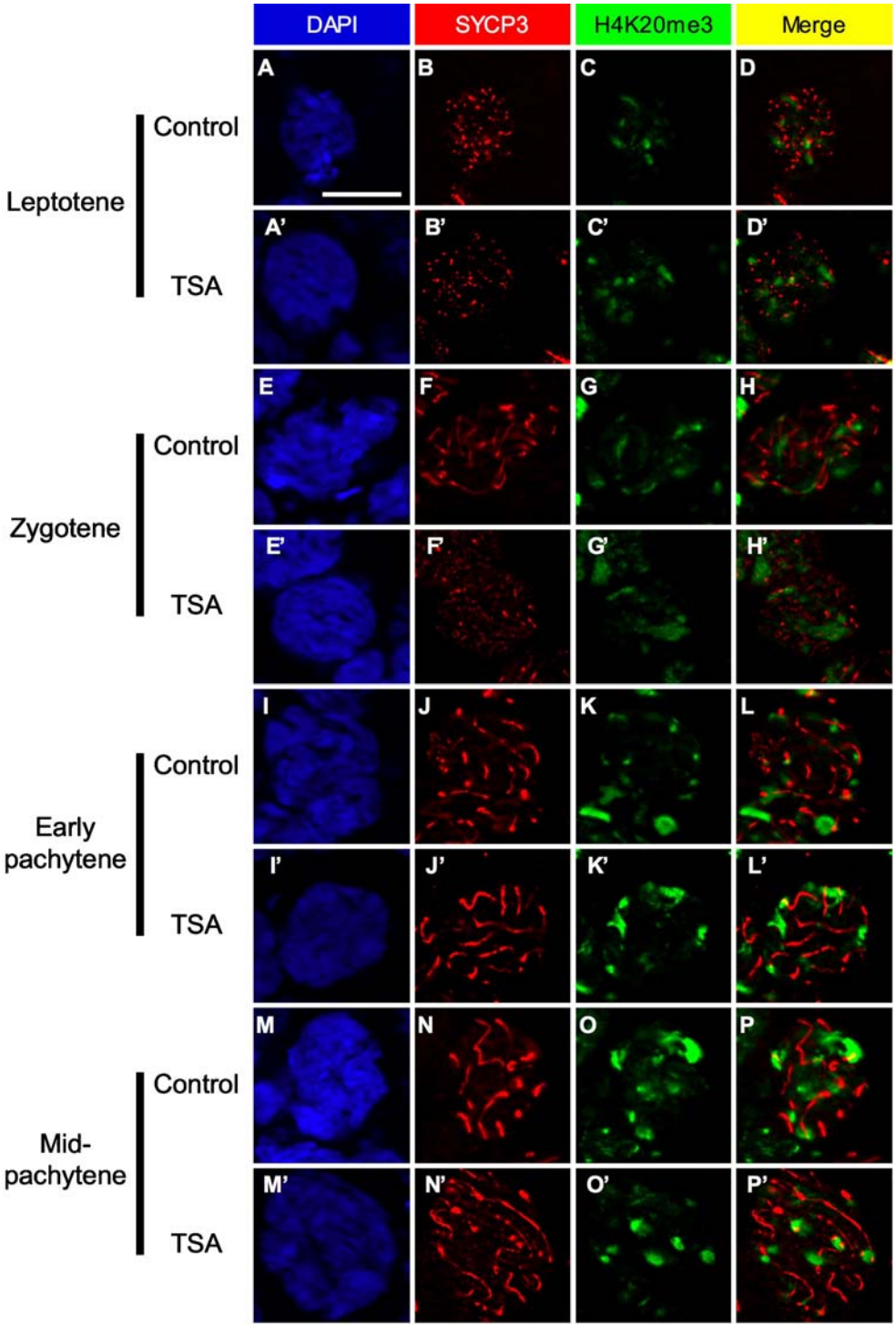

Fig. 4 Immunolocalization of histone mark H4K20me3 throughout meiotic prophase I of control and TSA-treated animals. SYCP3 immunodetection was used to indicate the SCs (*red*). Nuclei were stained with DAPI. **a–d** Leptotene cell from control animals. **a'**–**d'** Leptotene cell from TSA-treated animals. **e–h** Zygotene cell from control animals. **e'**–**h'** Zygotene cell from TSA-treated animals. **i–l** Early pachytene cell from control animals. **i'**–**l'** Early pachytene cell from TSA-treated animals. **m–p** Midpachytene cell from control animals. **m'**–**p'** Midpachytene cell from TSA-treated animals. The *bar* corresponds to 10 μm in all the optical sections

were unaffected (Fig. S2L). Therefore, we assumed that most of the observed meiotic cells were affected to some extend with the TSA treatment; however, we performed a statistical analysis to confirm whether there were alterations or not. These results corroborate that HDAC inhibition affects pachytene cells as reported by Steger's group (Fenic et al. 2004, 2008).

Dynamics of histone marks associated with the SC were altered after TSA treatment

To evaluate the effects of HDAC inhibition in the dynamics of histone marks associated with the SC, we decided to perform immunolabeling of H3K9me3, H3K27me3, and H4K20me3 throughout meiotic pro-

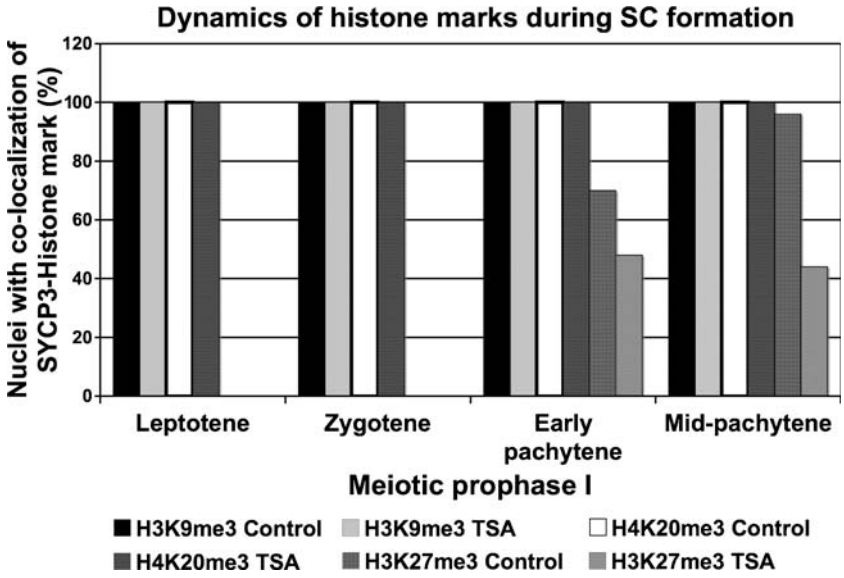

Fig. 5 Dynamics of histone marks during synaptonemal complex formation. Graphic showing the quantification of nuclei displaying colocalization of SYCP3 and histone marks H3K9me3, K3K27me3, and H4K20me3. A total of 150 nuclei per stage of meiotic prophase were observed

phase I. In TSA-treated animals, signals from H3K9me3 during leptotene cells were observed as foci that colocalized with the AEs (Fig. 2a'–d'). This distribution was similar to that found in the leptotene cells of control animals; however, the foci from H3K9me3 were faint and not as compact as in the control cells (compare Fig. 2d and d'). The pattern of this histone mark in zygotene, early pachytene, and midpachytene cells of treated animals was similar to that seen for the cells of the same stages in control animals but with the same less compact pattern observed in leptotene cells (Fig. 2e–h', i–l', and m–p', respectively). The signal pattern of H3K27me3 in TSA-treated animals was strikingly different to that observed in control cells. The signal was barely visible until midpachytene and did not colocalize with the SC (Fig. 3m'–p'). In contrast, the signal in control cells appeared in early pachytene, colocalized with the SC, and became more evident in midpachytene (Fig. 3i–p). The distribution of H4K20me3 throughout meiotic prophase I was the same for control and TSA-treated animals (Fig. 4).

The quantification indicates that the dynamics of H3K9me3 and H4K20me3 localization through meiotic prophase I was similar in control and TSA-treated animals in 100% of the analyzed nuclei (Fig. 5). However, the H3K27me3 signal in TSA-treated rats was barely visible at early pachytene and colocalized with the SC in 48% of analyzed nuclei, versus 70% colocalization in control cells (Fig. 5). The signal of this histone colocalized with the SC in a 44% of midpachytene cells of treated animals, as opposed to 96% in control cells (Fig. 5).

Taking these results into account, as well as statistical comparisons between control and TSA-treated cells, we summarize that the dynamics of H3K9me3 and H4K20me3 were not affected by HDAC inhibitor treatment. By contrast, H3K27me3 distribution was clearly affected.

Association of histone marks with the SC are affected after TSA treatment

Immunolabeling assays revealed a loss of colocalization of H3K27me3 in early and midpachytene and a blurry staining pattern of H3K9me3 after HDAC inhibition. Therefore, we decided to semiquantify the association of the different histone marks associated with the SC. To address this point, we immunoprecipitated the LEARS using anti-SYCP3 antibody as previously reported (Hernández-Hernández et al. 2008). Using this immunoprecipitated chromatin as template, we performed a second immunoprecipitation using antibodies against the different histone marks. By radioactive duplex PCR, we quantified the association of histone marks to the chromatin associated with LEs in control and TSA-treated cells (Fig. 6). Results were normalized with values obtained from amplification of DNA associated with acetylated histone H3, which is absent in LE. We employed an IgG-recognizing antibody as a mock control (Rincón-Arano et al. 2007). Analysis in control rats revealed that chromatin of LINE sequences, associated to the LE, was also preferentially associated with H4K20me3 (Fig. 6a–b), whereas chromatin of SINE and LTR sequences was associated with histone mark H3K27me3 (Fig. 6a–b). Finally, chromatin of satellite sequences was associated with LE and with H3K9me3 and H4K20me3 (Fig. 6a–b). Strikingly, association of all LEARS chromatin with the different histone marks was significantly diminished after the TSA treatment (Fig. 6a–b).

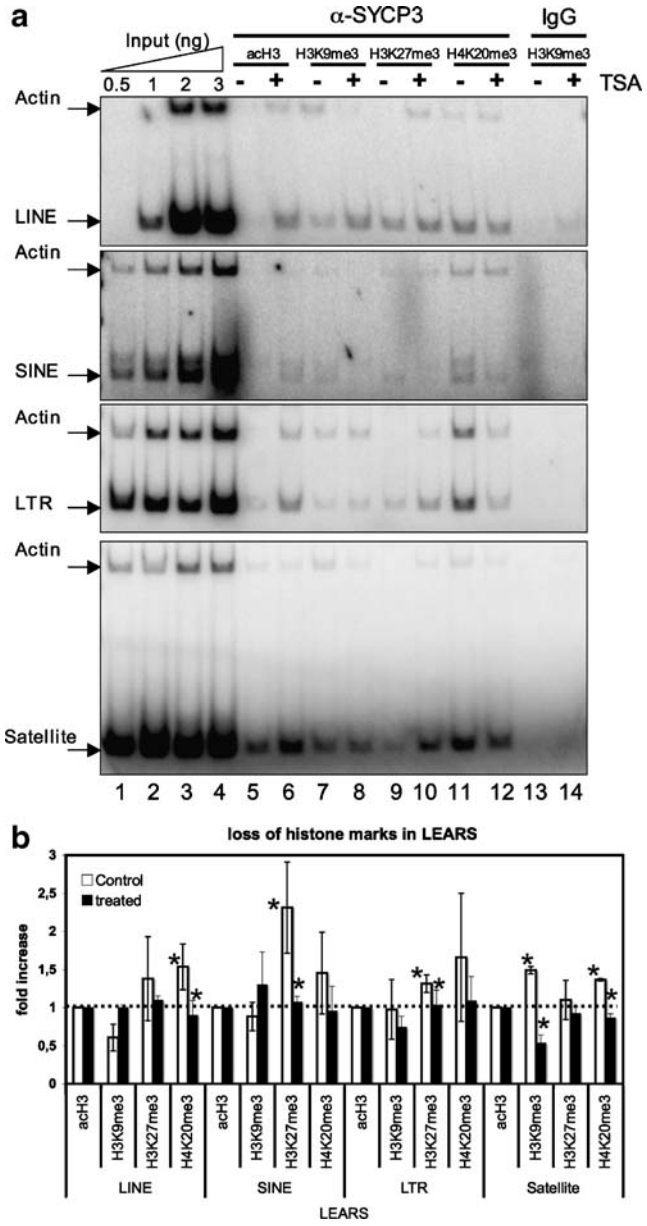

Fig. 6 TSA-mediated chromatin disruption affects the interaction of specific histone marks with LEARS and the LEs. Re-ChIP assay from untreated and TSA-treated rats. **a** In order to determine linear range amplification conditions, radioactive duplex PCR amplification of repeat sequences (*LINE*, *SINE*, *LTR*, and *Satellite* repeats), as well as the actin coding sequence (*Actin*) included as a control for relative quantification, was performed using increasing concentrations of genomic DNA (*Input*; *lanes 1–4*). Duplex PCR amplifications were then performed using as template DNA immunoprecipitated with anti-SYCP3 antibody and with the histone mark indicated in gonad tissue from control (*lanes 5*, *7*, *9*, *11*, and *13*) and treated rats (*lanes 6*, *8*, *10*, *12*, and *14*). **b** Data are shown as relative enrichment of the repeat sequence over the actin gene coding sequence, to which the value of one was obtained from the repeat/actin ratio in the input chromatin (*dotted line*). Results represent three independent immunoprecipitations. The *bars* represent the S.E. *Asterisks* show the significant in vivo interactions among SYCP3, repeat sequences, and epigenetic modifications in control rats (*white boxes*). The *asterisks on dark boxes* indicate the significant reductions of in vivo interactions after TSA treatment

These results support the observations of the immunolabeling assays and point out the relevance of HDACs for the incorporation and/or establishment of chromatin association to the SC.

Posttranscriptional histone modifications participate in the enrichment of DNA in the LE

We have found that H3K9me3, H3K27me3, and H4K20me3 are associated to the SC and that inhibition of HDACs induces the loss of colocalization with the SC. The loss of association of these histone marks with the SC also suggests the loss of DNA enrichment in the LE. To address this point, we performed ChIP in meiocytes of control and TSA-treated rats. In addition, we quantified the enrichment of the different kinds of repeat sequences associated to the LE as previously reported (Hernández-Hernández et al. 2008).

Our ChIP analyses revealed that TSA treatment did not affect the enrichment of LINE and satellite repeat sequences in SYCP3-associated chromatin. In contrast, the association of SINE and LTR sequences with the LE through SYCP3 appeared to be diminished (Fig. 7a–b), therefore suggesting that the inhibition of HDACs produced a loss in the incorporation of certain kind of DNA sequences to the LE. According to re-chIP and ChIP assays, we suggest that loss of SINE and LTR sequences from the LE is due to the failure in the trimethylation of lysine 27 of histone H3. However, the loss of enrichment of H3K9me3 and H4K20me3 from the LINE and LTR sequences did not produce a loss of this DNA in the LE, suggesting that these histone modifications are not needed for the incorporation of these sequences into the LE. Moreover, the presence of H3K9me3 and H4K20me3 (as seen in immunofluorescent assays) in the SC of meiocytes from control and TSA-treated animals suggest the presence of unidentified DNA sequences associated with the SC. Nevertheless, the loss of colocalization and loading of H3K27me3 to the SC, the loss of this histone from the SINE and LTR sequences, and the failure of incorporation of these LEARS to the SC point out a role for this histone mark in the SC structure.

To confirm the loss of DNA from the LE of the SC, we performed ultrastructural preferential DNA staining in midpachytene cell from control and treated rats (Fig. 8). Pachytene cells were determined according to the cellular association in the CSE in both control and treated rats. In a longitudinal view of control SCs, the DNA is visible inside of the LE in control animals (arrows in Fig. 8a, c) as previously reported (Ortiz et al. 2002). In TSA-treated pachytene cells, there was a drastic DNA staining decrease inside of the LE (arrowheads in Fig. 8b, d). This loss in the DNA specific staining pattern was present in 68% of the

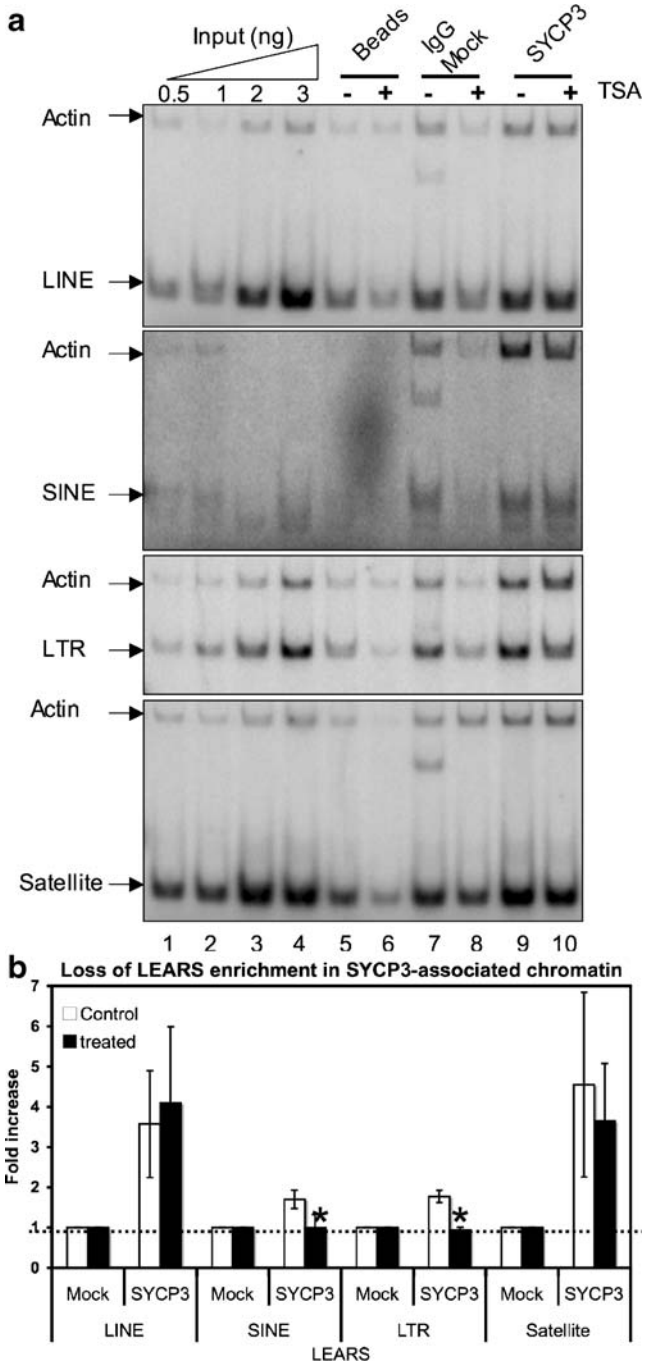

Fig. 7 TSA-mediated chromatin disruption affects the interaction of specific LEARS with the SC. Chromatin immunoprecipitation from untreated and TSA-treated rats. **a** To determine linear range amplification conditions, radioactive duplex PCR amplification of repeat sequences (*LINE*, *SINE*, *LTR*, and *satellite* repeats), as well as the actin coding sequence (*Actin*), included as a control for relative quantification, was performed using increasing concentrations of genomic DNA (*Input*; *lanes 1–4*). Duplex PCR amplifications were then performed using as template DNA immunoprecipitated with an anti-SYCP3 antibody in gonad tissue from control (*lane 9*) and treated rats (*lane 10*). An anti-IgG (*Mock*; *lanes 7* and *8*) and the immunoprecipitation reagent (*Beads*; *lanes 5* and *6*) were included as negative controls. **b** Data are shown as relative enrichment of the repeat sequence over the actin gene coding sequence, to which the value of one was obtained from the repeat/actin ratio in the input chromatin (*dotted line*). Results represent three independent immunoprecipitations. The *bars* represent the S.E. *Asterisks* show statistically significant differences in enrichment of the SYCP3-bound LEARS

analyzed nuclei (n=50). However, the signal did not completely disappear (arrows in Fig. 8b, d), suggesting a partial loss of association of DNA with the LE. These results were consistent with our ChIP assays, which showed that the associations of SINE and LTR sequences with the LE were lost, whereas the LINE and satellite sequences remained attached to the LE in TSA-treated rats (Fig. 7). Therefore, our observations support the idea that chromatin structure alteration via histone deacetylation inhibition affects the enrichment of a specific subset of repeat DNA sequences in the LE and perhaps affecting the SC structure.

SC structure is altered after HDAC inhibition

Our results suggest that H3K27me3 is important for the enrichment of SINE and LTR sequences to the LE of the SC. To evaluate whether the loss of association between the DNA of LEARS and the LE affects SC structure, we immunolocalized the proteins of the LE and the central region (CR) of the SC. Gonad tissue sections obtained from control and treated rats were stained with antibodies against SYCP3 and SYCP1 (Fig. 9). Control sections showed a normal seminiferous tubule structure (Fig. 9a–d), in contrast to seminiferous tubules where the structure was affected by the presence of pachytene cells at the lumen of the tubule (Fig. 9l–o). This distribution was observed in 64% of the treated tubules in stages IX–XI of the CSE (data no shown). SCs of control sections show normal association of SYCP1 and SYCP3, clearly indicating that the integrity of the SC structure was preserved (Fig. 9e–k). In sections of treated rats, many SCs contained discontinuities in their staining patterns (Fig. 9p–v). The signal of SYCP1 was discontinuous (arrowheads in Fig. 9u, v), while SYCP3 staining remained uniform (arrows in Fig. 9t, v). This suggests a partial failure in SC structure associated with chromatin structural defects and CR dissociation. To evaluate this possibility, we followed the staining pattern of SYCP3 and SYCP1 throughout zygotene, early, and midpachytene. At leptotene stage, the newly formed AEs were similar in cells of control and treated rat (as seen in Figs. 2, 3, and 4). At zygotene stage, the AEs in control rats were thicker than in leptotene stage due to initiation of synapsis between the AEs of the homologous chromosomes, whereas in zygotene of TSA-treated tubules, the AEs are thinner compared with the AEs of control cells, suggesting a delay in the synapsis initiation (Fig. 10a, a').

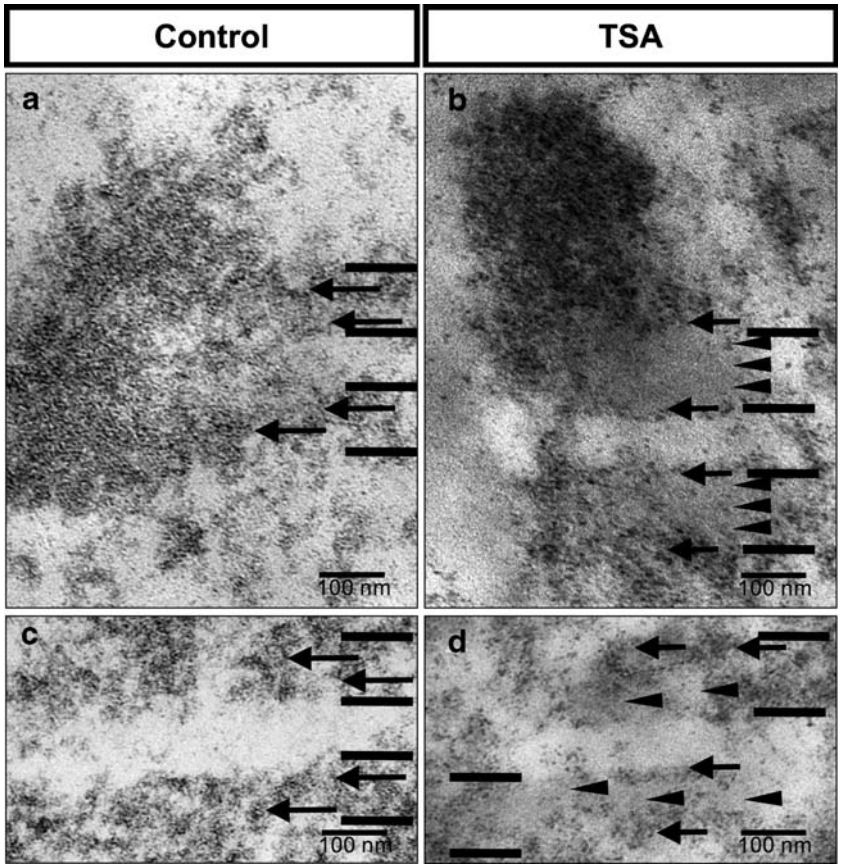

Fig. 8 Electron micrographs of SCs visualized by preferential DNA staining. **a** and **c** SC of midpachytene cell from control rat. The DNA is seen as a network (*arrows*) within the LE (indicated by *parallel lines*). **b** and **d** SC of midpachytene cell from TSA-treated rat. The DNA in long stretches of LE appears diffuse (*arrowheads*). The *bar* represents 100 nm

Only 12% of analyzed nuclei displayed normal LE maturation in zygotene cells of treated animals, compared to 98% of control nuclei (Fig. 10j). Towards early and midpachytene, the LEs in both control and treated seminiferous tubules were identical (Fig. 10d, d', g, g', and j), supporting the accurate maturation of the LE. The CR, as indicated by SYCP1 staining, was first visible in zygotene cells of control and treated animals (Fig. 10b, b') in 100% of the cases (Fig. 10k). At early pachytene, SYCP1 staining completely colocalized with the LE in 100% of analyzed control and treated cells (Fig. 10e, e', and k). Noticeably, at midpachytene of TSA-treated animals, the staining pattern of SYCP1 had interruptions (Fig 10i'). Only 37% of treated midpachytene cells had a normal CR staining pattern (Fig. 10k), whereas midpachytene cells of control animal had 96% (Fig. 10k). These results suggest that under HDAC inhibition, there is a delay in the formation of the LE at zygotene stage. Nonetheless, this delay occurs without affecting synapsis initiation. In fact, synapsis was accomplished at early pachytene at the time that the signals for SYCP3 and SYCP1 were completely colocalized, but by midpachytene, there is a loss in the CR structure.

With the aim of determining the ultrastructural abnormalities of the SC, we analyzed serial sections of midpachytene cells from TSA-treated rat gonads by electron microscopy. We found 78% of nuclei contained unpaired and fragmented LEs at midpachytene (n=150, Fig. 11 T), and when discernible, 42% of the SC (n=100 SCs) displayed an altered CR structure (Fig. 11), manifested as gaps in the CR or incomplete CR between paired chromosomes. These alteration were present in 76% and 24% of the analyzed SC, respectively (n=42 SCs, Fig. 11 T). For example, in serial section 1, the SC appears as a tripartite structure (arrows Fig. 11, s1). In section 2, the SC undergoes a separation of LEs at one extreme and the CR is no longer visible. The two separated LEs are anchored to the NE (arrows in Fig. 11, s2). The other end of the SC is also anchored to the NE (arrows in Fig. 11, s3–s7). The altered SC structure is more evident by a superimposition of all slides (Fig. 11, 3D). These results show ultrastructural defects in the SC structure of TSA-treated rat gonad. Thus, TSA-mediated HDAC inhibition correlates with partially altered SC structure that is presumably caused, at least in part, by chromatin configuration defects and loss of DNA attachment to the LEs.

Double strand break repair process is not affected by HDAC inhibition

SC formation can be affected by failures in DNA double strand break induction (DSB) or repair (Vallente et al. 2006; Bolcun-Filas et al. 2007). Therefore we monitored the

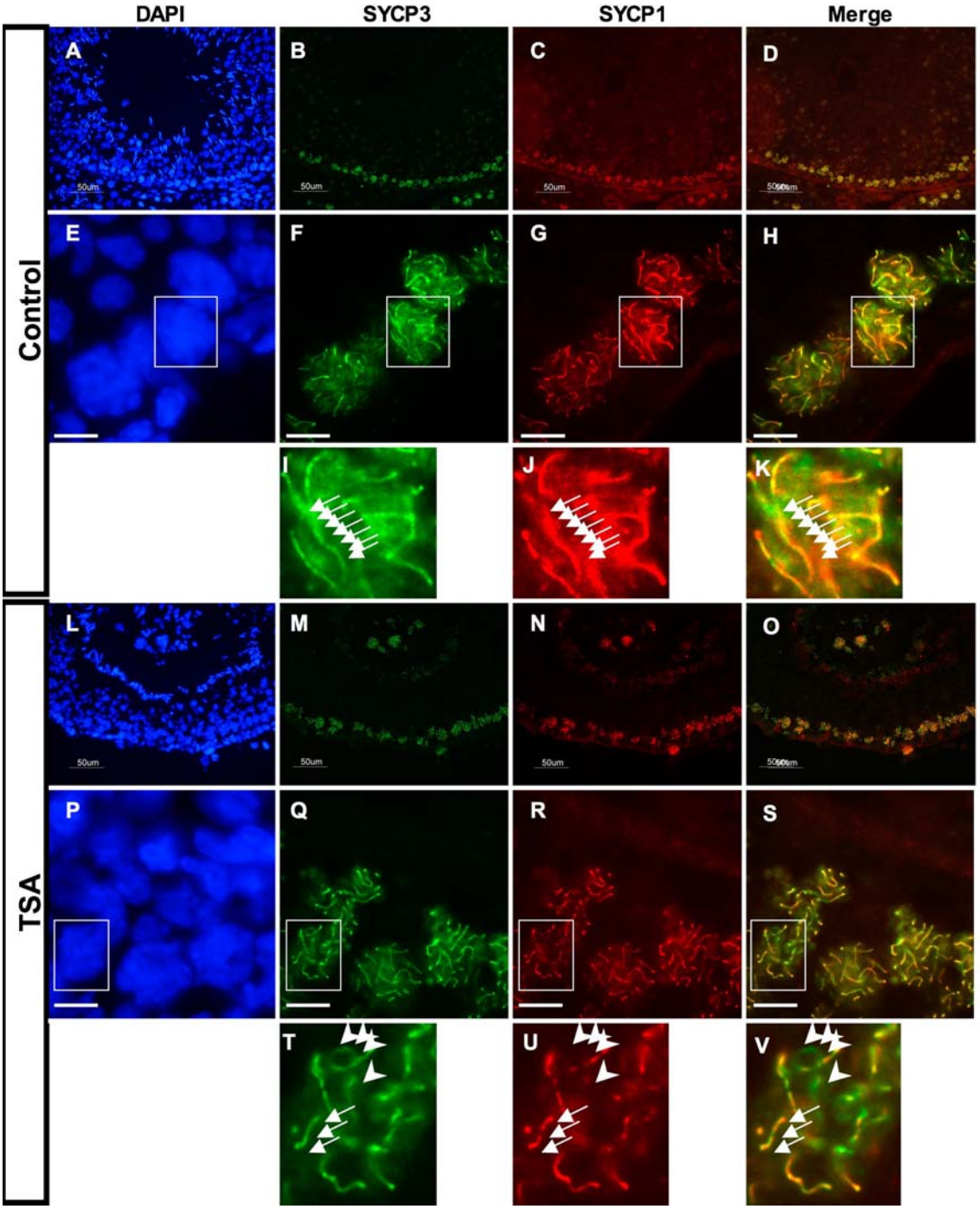

Fig. 9 Immunofluorescence of SYCP3 and SYCP1 in sections of gonad tissue of control and TSA-treated rats. **a–k** Control rats, **l–v** treated rats. **a–d** Normal morphology of seminiferous tubule. The *bar* represents 50 μm (50 um). **a** and **e** Cell nuclei were stained with DAPI, and SC components were visualized by SYCP3 (*green*) and SYCP1 (*red*) staining. Colocalization signals in *yellow* (*merge*) are shown. **i–k** Digital zooms of insets in **f–h**, respectively, showing the continuous signals of SYCP3 and SYCP1 and their colocalization (*arrows*). The *bar* in **e–h** represents 10 μm. **l–o** Pachytene cells were visible in the lumen of the seminiferous tubules in TSA-treated rats. **l** and **p** Pachytene nuclei were stained with DAPI, and SC components were visualized by SYCP3 (*green*) and SYCP1 (*red*) staining. Colocalization signals in *yellow* are shown (*merge*). **t–v** Digital zooms of insets in **q–s**, respectively, showing the continuous signals of SYCP3 and SYCP1, their colocalization (*arrows*) and the discontinuities in SYCP1 signal (*arrowheads*). The *bar* in **p–s** represents 10 μm

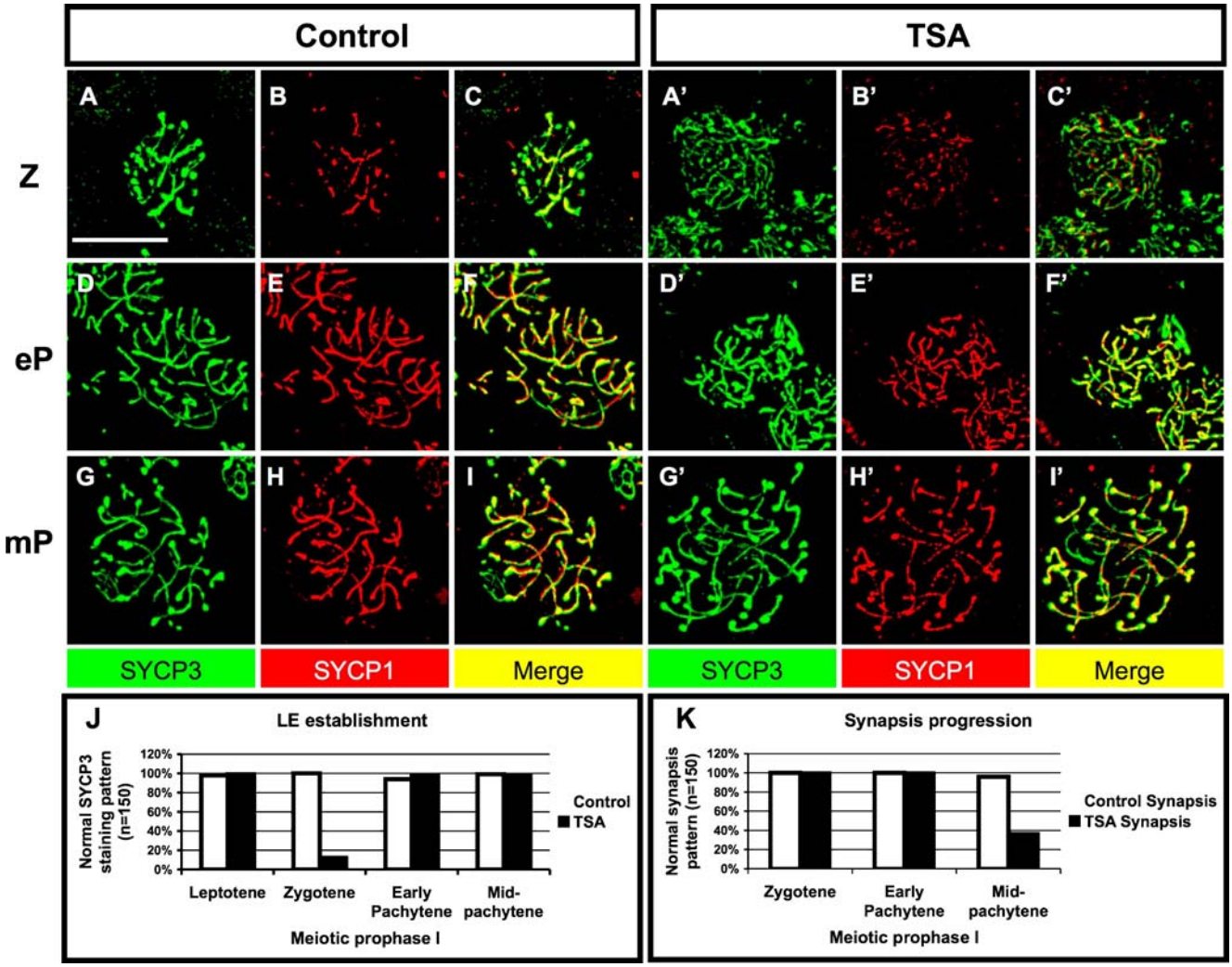

Fig. 10 Z-Stack from optical sections. LEs were stained using SYCP3 antibody (*green*), and synapsis was observed by immunolocalization of SYCP1 protein (*red*). **a–c** Zygotene cell (*Z*) from control animal. **a'–c'** Zygotene cell from TSA-treated animal. **d–f** Early pachytene cell (*eP*) from control animal. **d'–f'** Early pachytene cell from TSA-treated rat. **g–i** Midpachytene cell (*mP*) from control rat. **g'–i'** Midpachytene cell from TSA-treated rat. The *bar* represents 10 μm. **j** Graphic showing the percentages of nuclei (n=150) that displayed normal SYCP3 staining pattern from leptotene until midpachytene cells from control and TSA-treated animals. **k** Graphic showing the percentages of nuclei (n=150) that displayed normal SYCP1 staining pattern from zygotene until midpachytene cells from control and TSA-treated animals

presence of the phosphorylated histone variant H2AX (H2AXγ), which is recruited to DNA DSBs in response to damage. The signal of H2AXγ was present in 98% (n=100) of the zygotene cells from control animals (Fig. 12a and b) and 94% (n=100) of the zygotene cells from TSA-treated rats (Fig. 12c and d) when the SC was being formed (Fig. 12a–d). Furthermore, histone H2AXγ was relocated to the heterochromatin of the XY body in 100% of the analyzed pachytene cells from control rats, as expected (Fig. 12e and f). Moreover, in 79% (n=100) of the pachytene cells of treated animals, H2AXγ was not present in the sexual chromosomes, and there was no visible XY body (Fig. 12g and h), suggesting failures in the formation of the heterochromatin of the XY body. This result provides additional evidence of the effects of TSA treatment on heterochromatin formation.

Furthermore, DMC1 is a meiotic repair protein that is loaded onto DSBs during leptotene–zygotene stages and removed at pachytene stage. We found that the DMC1 signal was present in 94% and 98% (n=100) of zygotene cells in control (Fig. 12i and j) and TSA-treated rats, respectively (Fig. 12k and l). At pachytene stages, the signal of DMC1 was no longer visible in either case (Fig. 12m–p), supporting the normal progression of the DSB repair process. Taken together, these results confirm that the failure in the SC structure is due to the dissociation of LEARS from the SC and is not due to failures in other pathways, such as DNA DSB induction or repair.

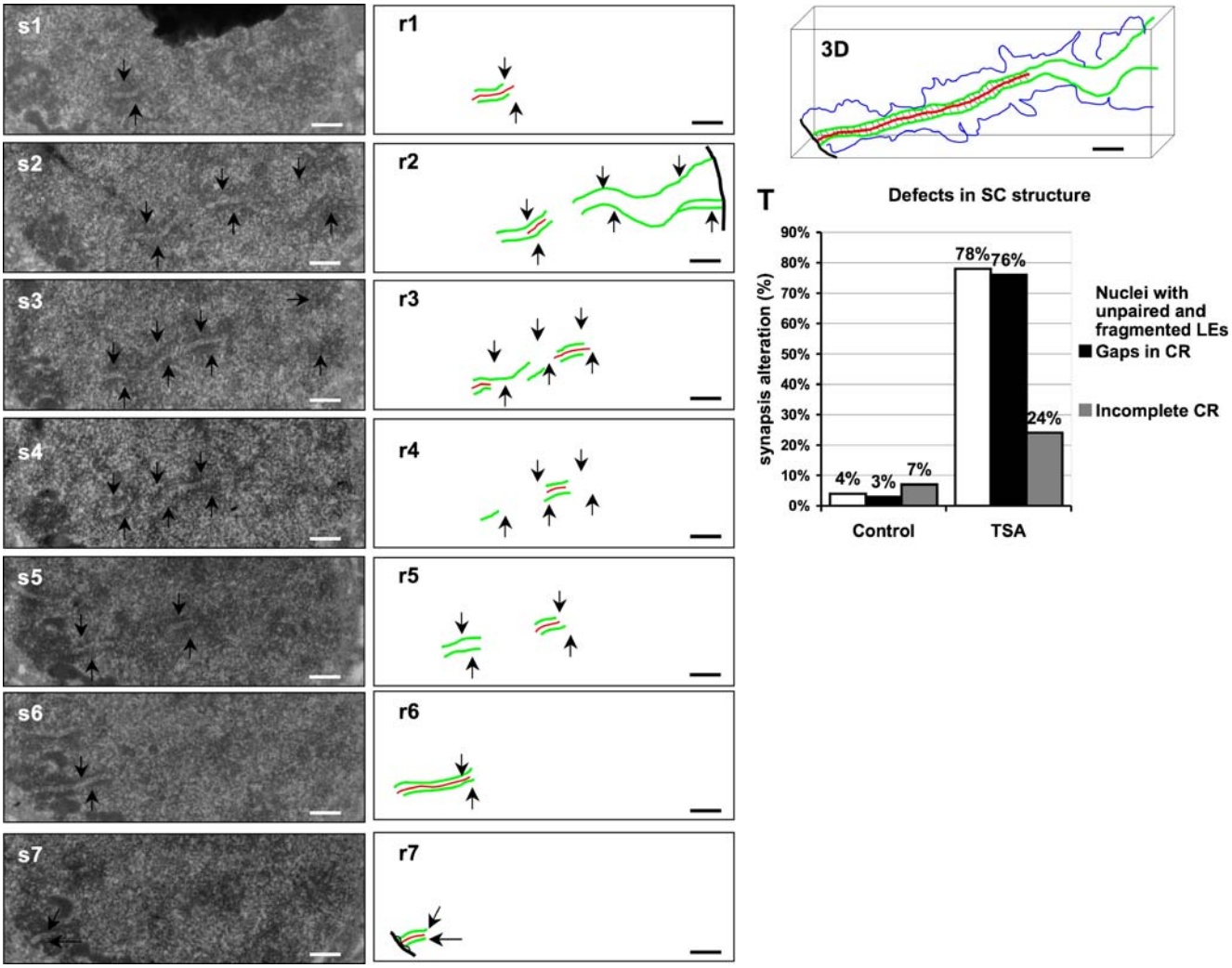

Fig. 11 3D reconstitution of a SC in a TSA-treated rat. Serial sections 1–7 (*s1–s7*) correspond to electron micrographs of an altered SC in a midpachytene cell. *Arrows* show the SC in the different sections. *r1–r7* Drawings of the SC (*arrows*) in the serial sections. Lateral elements are shown in *green*, whereas the central region is in *red*. The drawings in *r1–r7* were merged to reconstruct (*3D*) the altered SC attached to the nuclear envelope. The *bar* represents 500 nm. *T* Graphics showing the defects in the SC at ultrastructural level. A total of 150 nuclei in midpachytene stage and 100 SCs were observed in both control and TSA-treated rats

In summary, our results indicate that H3K9me3 and H4K20me3 colocalize with the AEs from the beginning of meiotic prophase and until pachytene stage with SC extremities (Fig. 13). Remarkably, H3K27me3 appeared to colocalize with long fragments of the SC at early pachytene, and this colocalization became more so evident in midpachytene cells (Fig. 13), suggesting a role of this histone mark in the establishment of the mature SC. Interference of histone methylation by HDAC inhibition produced a loss of H3K27me3 and its associated DNA in the SC (Fig. 13). Furthermore, H3K9me3 and H4K20me3 histone marks were associated with LINE and satellite sequences in control animals. However re-ChIP analyses showed a significant loss of this histone mark from the LE-associated chromatin after HDAC inhibition, but LINE and Satellite sequences remain attached to the SC, thus, suggesting a distinct epigenetic code to attach this DNA to the LE. Further, unchanged colocalization of H3K9me3 and H4K20me3 in the chromosome ends of the SC from treated cells points out the association of uncharacterized DNA sequences to the SC.

Discussion

In the organisms that undergo sexual reproduction, meiotic recombination represents a central process in which chromatin structure, the synaptonemal complex, and epigenetic components play an active role. In this work, we have characterized the histone posttranslational modifications that are present in lateral element-associated repeat sequences. We performed immunolocalization of H3K9, H3K27,

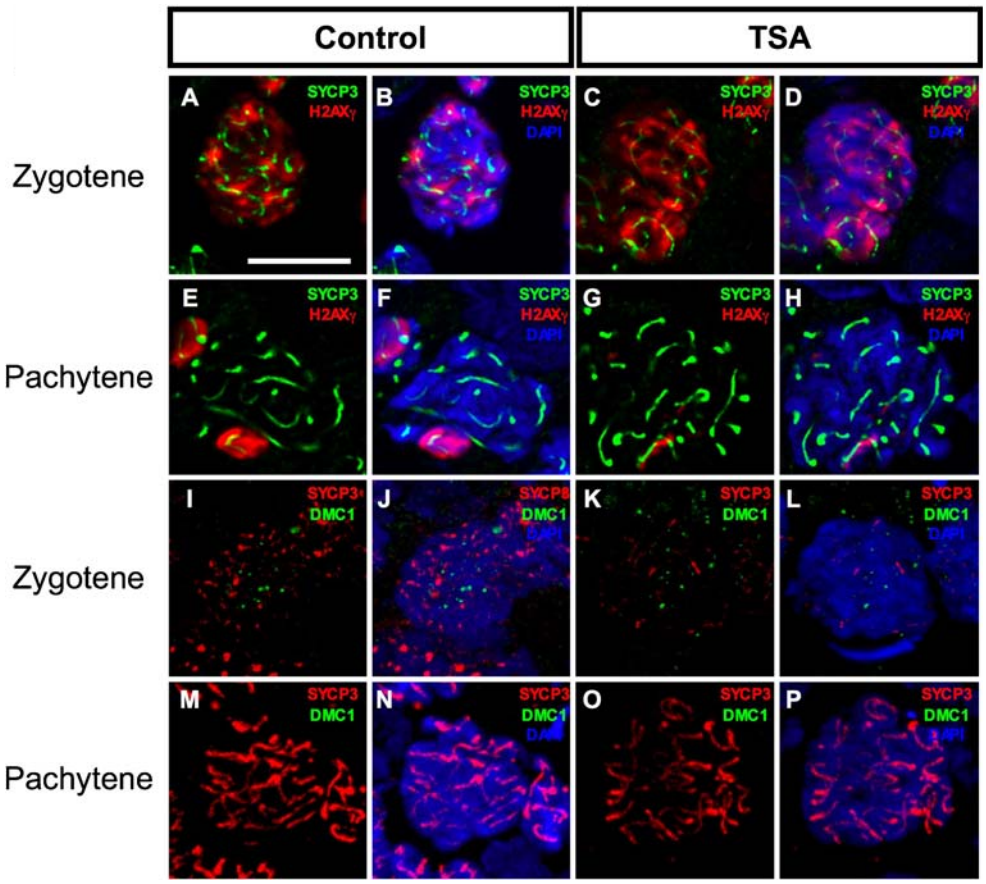

Fig. 12 Optical sections of zygotene and pachytene cells. **a–h** Immunofluorescence for H2AXγ (*red*) plus SYCP3 (*green*) in zygotene and pachytene cells of control and TSA-treated rats. **i–p** Z-stack of optical sections for nuclei with immunofluorescence for DMC1 (*green*) plus SYCP3 (*red*) in zygotene and pachytene cells of control and TSA-treated rats. The *bar* represents 10 μm

and H4K20 mono-, di-, and trimethylated states throughout meiotic prophase I of rat. We found that colocalization of SYCP3 and H3K27me3 is important for the SC structure. The H3K9me3 distribution near the periphery of the prepachytene nucleus resembles the association of telomeric sequences with the NE (Viera et al. 2003). This mark was already present in the telomeres of chromosomes at leptotene stage (Fig. 2a–d) and persisted even after the assembly of the SC (Fig. 2m–p). H4K20me3, which marks constitutive and facultative heterochromatin (Benetti et al. 2007), was detected since leptotene stage and had the same dynamics as H3K9me3 (Fig. 4). Conversely, H3K27me3, which is found in constitutive or facultative heterochromatin (Barski et al. 2007; Benetti et al. 2007), appeared at early pachytene stage colocalized with the SC and toward midpachytene; this histone mark colocalized with regions of the SC (Fig. 3). These distribution patterns, in addition to the fact that H3K9me3 interacts with SYCP3 in LINE sequences in vivo, suggest that this mark could be relevant for SC formation. This idea is further supported by studies where knockdown of the Suv39h and G9a histone methyltransferases caused synapsis failure between homologous chromosomes (Peters et al. 2001; Tachibana et al. 2007). Similarly, H4K20me3 appeared in leptotene cells and colocalized with the ends of the SC at pachytene stage. Therefore, this mark could also play a role in SC formation (Fig. 4). Indeed, chromatin that incorporates this modified histone interacts in vivo with LINE and satellite sequences through SYCP3 (Fig. 6).

The H3K27me3 distribution during pachytene stage, and its absence during prepachytene stages, represents one of the most relevant findings of our investigation. At the time when the SC matures at the pachytene stage, this histone

Histone mark associated to SC precursors throughout the meiotic prophase I (%)									Association with LEARS		Effects in SC after TSA-treatment
Histone mark	Axial Elements (presence)		Lateral Elements (presence)		Lateral Elements of mature SC (presence)						
	Leptotene		Zygotene		Early pachytene		Mid-pachytene				
	TSA-treatment								TSA Treatment		
	-	+	-	+	-	+	-	+	-	+	
H3K9me3	100	100	100	100	100	100	100	100	Satellite-	----	-Loss of DNA from the LE of the SC, mainly SINE- and LTR-sequences
H4K20me3	100	100	100	100	100	100	100	100	LINE- Satellite-	---- ----	-Altered SYCP1 staining pattern
H3K27me3	0	0	0	0	70	48	96	44	SINE- LTR-	---- ----	-Absences of CR between aligned LEs

Fig. 13 Summarized results. Histone modification marks associated to the SC and their dynamics throughout meiotic prophase I. Percentages of colocalization with the SC during the meiotic prophase I in nuclei from control and TSA-treated rats. Also, the effect of TSA treatment in the association of histone marks with the LEARS and the effect of treatment in the SC structure

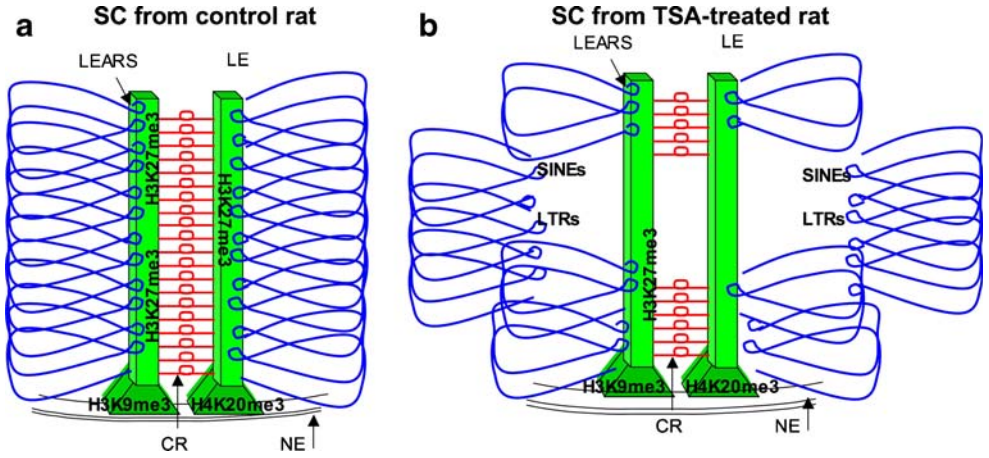

Fig. 14 Model of SC structure in control and TSA-treated rats. a SC of a control rat. The chromatin of homologous chromosomes is anchored to the lateral elements (*LE*) through lateral elements-associated repeat sequences (*LEARS*), for which chromatin structure is dictated by histone posttranslational modifications like H3K9me3, H3K27me3, and H4K20me3. **b** Upon inhibition of histone deacetylases, the presence of H3K27me3 in SINE and LTR sequences decreases dramatically, which could favor detachment of such sequences from the LEs. This is accompanied by alteration of the SC's central region (*CR*)

mark is incorporated into large domains of the LEs (Fig. 3). SINEs and LTRs were the only LEARS associated with this histone mark, which is remarkably lost after TSA treatment. These data suggest that H3K27me3 in SINE and LTR sequences is a prerequisite for their incorporation in the SC, which is consequently abolished when the disruption of chromatin structure is induced (Fig. 7). This could also explain the partial DNA loss in the LEs (Figs. 7 and 8).

We found that H4K20me3 is enriched in LINE sequences that form part of the LEARS and that this histone mark is disturbed after TSA treatment without affecting the association of LINE sequences with the SC (Figs. 6 and 7). The same phenomenon was seen for satellite sequences, which are enriched in H3K9me3 and H4K20me3 (Figs. 6 and 7). However, loss of H3K9me3 from LINE sequences, and H3K9me3 and H4K20me3 from satellite sequences, does not affect their attachment to the LEs, suggesting that a unidentified histone mark could be involved in the attachment of these sequences to LEs. On the other hand, H3K27me3 seems to be critical for maintaining the association of SINE and LTR sequences with the LE.

Colocalization of H3K27me3 with the SC is lost upon TSA-mediated disruption of chromatin structure in rats. However, the cytological distribution of H3K9me3 and H4K20me3 was not affected after TSA treatment (Figs. 2 and 4); notwithstanding, such marks were decreased in LINE and satellite sequences, respectively (Fig. 6). Neither LINE nor satellite sequences lost the attachment to SYCP3 protein (Fig. 7). Therefore, it seems unlikely that the diminishment of H3K9me3 and H4K20me3 in LINE and satellite sequences interferes with their incorporation in the SC. The cytological distribution of these marks is perhaps not affected because they are present in constitutive telomeric heterochromatin, which is composed mainly of telomeric DNA repeats. Further studies are needed to elucidate the mechanisms by which all the LEARS are recruited to the SC.

Given all of these results, we suggest a model in which the LE's chromatin composition may play a central role in SC formation and structure (Fig. 14). In such a model, H3K9me3 and H4K20me3 are associated with the end of the SC (Fig. 14a), presumably with the telomeric domain and the region involved in anchorage to the NE. While H3K27me3 is present along extended tracts of the LE (Fig. 14a), this histone mark preferentially associates with SINE and LTR sequences. The destabilization of this histone mark produces detachment of chromatin from the LEs, mainly SINE and LTR repeat sequences, while the association of H3K9me3 and H4K20me3 with the extremity of the SC by SYCP3 is not altered (Fig. 14b). This is accompanied by alteration of the CR of the SC.

It has been shown that in budding yeast meiosis, chromatin modifications at meiotic hot spots are needed for the correct progression of DSB repair (Yamashita et al. 2004). Further, a relaxed chromatin structure is necessary for DSB initiation at meiotic hot spots (Merker et al. 2008; Borde et al. 2009). It has also been shown that the H3K4me3 epigenetic mark, which is a characteristic of open chromatin, allows for correct DSB formation (Borde et al. 2009). In mammals, this methylation of H3K4 is upregulated at the time that DSBs are produced and downregulated between zygotene and pachytene stages, suggesting that a dynamic chromatin structure is indeed important for DSBs and subsequent repair processes (Godmann et al. 2007). Moreover, H3K4me3 has to be demethylated to allow the correct formation of the SC by

the incorporation of CR-specific proteins (Prieto et al. 2009). These results point out the relevance of posttranscriptional histone marks in the SC formation through meiotic prophase I. Our results show that H3K27me3 appears at early pachytene stage, colocalizes with the SC, and most importantly, that indirect inhibition of this epigenetic mark produces defects in SC structure. Therefore, we have generated evidence that supports the involvement of chromatin structure in SC formation and/or establishment. Further, H3K27 hyperacetylation creates increased meiotic recombination at one specific hot spot in budding yeast meiosis, suggesting that regulation of this posttranscriptional histone modification is important for meiotic recombination (Merker et al. 2008). Incorporation of meiotic hot spots to the LE of the SC (Hernández-Hernández et al. 2008, 2009) could be due to a trimethylation of H3K27 following deacetylation, thereby explaining H3K27me3 colocalization with the SC at early pachytene. It is clear that chromatin structure is important for SC formation, for establishment, and for correct meiotic recombination. However, this field has been addressed recently, and many perspectives have been raised, making it an interesting topic to be studied. Our work provides evidence of such interplay, and we are currently addressing some of the questions raised by our results.

Previous studies have shown that treatment of mice with the histone deacetylase inhibitor TSA impairs meiosis at two points: in the pachytene stage and in spermatids (Fenic et al. 2004). Recently the same research group has shown that pachytene cell death did not originate from down-regulation of meiosis-specific genes (Fenic et al. 2008). Our results support the idea that the damage in pachytene cells is induced by alteration of specific epigenetic patterns associated with the LEARS.

Acknowledgments We thank Sidney Carter, Catherine M. Farrell, and Paul Delgado-Olguín for critical reading of the manuscript and suggestions. We would like to thank members of our research group for stimulating scientific discussions and suggestions. AHH is a fellowship recipient from the Posgrado en Ciencias Biológicas, CONACyT (181375). This work was supported by grants from the Dirección General de Asuntos del Personal Académico—UNAM (IN209403 and IN214407) and Consejo Nacional de Ciencia y Tecnología-CONACyT (42653-Q and 58767) to FRT. CONACyT (81213), DGAPA-PAPIIT (IN203308-3) to GHVN. We also acknowledge the excellent technical assistance of Georgina Guerrero Avendaño.

References

Adler ID (1996) Comparison of the duration of spermatogenesis between male rodents and humans. Mutat Res 352:169–172

Barski A, Cuddapah S, Cui K, Roh TY, Schones DE, Wang Z, Wei G, Chepelev I, Zhao K (2007) High-resolution profiling of histone methylations in the human genome. Cell 129:823–837

Benetti R, García-Cao M, Blasco MA (2007) Telomere length regulates the epigenetic status of mammalian telomeres and subtelomeres. Nat Genet 39:243–250

Bolcun-Filas E, Costa Y, Speed R, Taggart M, Benavente R, De Rooij DG, Cooke HJ (2007) SYCE2 is required for synaptonemal complex assembly, double strand break repair, and homologous recombination. J Cell Biol 176:741–747

Borde V, Robine N, Lin W, Bonfils S, Géli V, Nicolas A (2009) Histone H3 lysine 4 trimethylation marks meiotic recombination initiation sites. EMBO J 28:99–111

Clermont Y (1972) Kinetics of spermatogenesis in mammals: seminiferous epithelium cycle and spermatogonial renewal. Physiol Rev 52:198–236

Cogliati R, Gautier A (1973) Mise en évidence de l'ADN et des polysaccharides á l'aide d'un nouveau réactif de type Schiff. C R Acad Sci D 276:3041–3044

Godmann M, Auger V, Ferraroni-Aguiar V, Di Sauro A, Sette C, Behr R, Kimmins S (2007) Dynamic regulation of histone H3 methylation at lysine 4 in mammalian spermatogenesis. Biol Reprod 77:754–764

Ekwall K, Olsson T, Turner BM, Cranston G, Allshire RC (1997) Transient inhibition of histone deacetylation alters the structural and functional imprint at fission yeast centromeres. Cell 91:1021–1032

Fenic I, Hossain HM, Sonnack V, Tchatalbachev S, Thierer F, Trapp J, Failing K, Edler KS, Bergmann M, Jung M, Chakraborty T, Steger K (2008) In vivo application of histone deacetylase inhibitor trichostatin-A impairs murine male meiosis. J Androl 29:172–185

Fenic I, Sonnack V, Failing K, Bergmann M, Steger K (2004) In vivo effects of histone-deacetylase inhibitor trichostatin-A on murine spermatogenesis. J Androl 25:811–818

National Research Council (NRC) (1996) Guide for the care and use of laboratory animals. The National Academy Press, Washington DC

Hernández-Hernández A, Rincón-Arano H, Recillas-Targa F, Ortiz R, Valdes-Quezada C, Echeverría OM, Benavente R, Vázquez-Nin GH (2008) Differential distribution and association of repeat DNA sequences in the lateral element of the synaptonemal complex in rat spermatocytes. Chromosoma 117:77–87

Hernández-Hernández A, Vázquez-Nin GH, Echeverría OM, Recillas-Targa F (2009) Chromatin structure contribution to the synaptonemal complex formation. Cell Mol Life Sci 66:1198–1208

Khalil AM, Boyar FZ, Driscoll DJ (2004) Dynamic histone modifications mark sex chromosome inactivation and reactivation during mammalian spermatogenesis. Proc Natl Acad Sci USA 101:16583–16587

Martens JHA, O'Sullivan RJ, Braunschweig U, Opravil S, Radolf M, Steinlein P, Jenuwein T (2005) The profile of repeat-associated histone lysine methylation states in the mouse epigenome. EMBO J 24:800–812

Merker JD, Dominska M, Greenwell PW, Rinella E, Bouck DC, Shibata Y, Strahl BD, Mieczkowski P, Petes TD (2008) The histone methylase Set2p and the histone deacetylase Rpd3p repress meiotic recombination at the HIS4 meiotic recombination hotspot in *Saccharomyces cerevisiae*. DNA Repair 7:1298–1308

Ortíz R, Echeverría OM, Ubaldo E, Carlos A, Scassellati C, Vázquez-Nin GH (2002) Cytochemical study of the distribution of the RNA and DNA in the synaptonemal complex of guinea-pig and rat spermatocytes. Eur J Histochem 46:133–142

Page SL, Hawley RS (2004) The genetics and molecular biology of the synaptonemal complex. Annu Rev Cell Dev Biol 20:525–558

Peters AH, O'Carroll D, Schertan H, Mechtler K, Sauer S, Schöfer C, Weipoltshammer K, Pagani M, Lachner M, Kohlmaier A, Opravil S, Doyle M, Sibilia M, Jenuwein T (2001) Loss of the

Suv39h histone methyltransferases impairs mammalian heterochromatin and genome stability. Cell 117:323–337

Prieto I, Kouznetsova A, Fütterer A, Trachana V, Leonardo E, Alonso Guerrero A, Cano Gamero M, Pacios-Bras C, Leh H, Buckle M, Garcia-Gallo M, Kremer L, Serrano A, Roncal F, Albar JP, Barbero JL, Martínez-A C, van Wely KH (2009) Synaptonemal complex assembly and H3K4Me3 demethylation determine DIDO3 localization in meiosis. Chromosoma 118:617–632

Rincón-Arano H, Furlan-Magaril M, Recillas-Targa F (2007) Protection against telomeric position effects by the chicken cHS4 β-globin insulator. Proc Natl Acad Sci USA 104:14044–14049

Tachibana M, Nozaki M, Takeda N, Shinkai Y (2007) Functional dynamics of H3K9 methylation during meiotic prophase progression. EMBO J 26:3346–3359

Vallente RU, Cheng EY, Hassold TJ (2006) The synaptonemal complex and meiotic recombination in humans: new approaches to old questions. Chromosoma 115:241–249

Viera A, Parra MT, Page J, Santos JL, Rufas JS, Suja JA (2003) Dynamic relocation of telomere complexes in mouse meiotic chromosomes. Chromosome Res 11:797–807

Yamashita K, Shinohara M, Shinohara A (2004) Rad6-Bre1-mediated histone H2B ubiquitylation modulates the formation of double-strand breaks during meiosis. Proc Natl Acad Sci USA 101:11380–11385